FEMS Microbiology Ecology, 94, 2018, fiy144

doi: 10.1093/femsec/fiy144
Advance Access Publication Date: 28 July 2018
Research Article

RESEARCH ARTICLE

Freshwater copepod carcasses as pelagic microsites of dissimilatory nitrate reduction to ammonium

Peter Stief[1,*], Ann Sofie Birch Lundgaard[1], Alexander H. Treusch[1], Bo Thamdrup[1], Hans-Peter Grossart[2] and Ronnie N. Glud[1,3]

[1]Department of Biology, Nordcee, University of Southern Denmark, Campusvej 55, 5230 Odense M, Denmark, [2]Institute of Freshwater Ecology and Inland Fisheries, Department of Limnology of Stratified Lakes, Alte Fischerhütte 2, 16775 Neuglobsow, Germany and [3]Department of Ocean and Environmental Sciences, Tokyo University of Marine Science and Technology, 108–8477 Tokyo, Japan

*Corresponding author: Department of Biology, Nordcee, University of Southern Denmark, Campusvej 55, 5230 Odense M, Denmark. Tel: +45 65507980; E-mail: peterstief@biology.sdu.dk

One sentence summary: Freshwater copepods, such as *Eudiaptomus* sp., host unique microenvironments in the water column of lakes and thereby enable diverse anaerobic nitrate conversion pathways mediated by bacterial reductases.

Editor: Lee Kerkhof

ABSTRACT

A considerable fraction of freshwater zooplankton was recently found to consist of dead specimens that sink to the lake bottom. Such carcasses host intense microbial activities that may promote oxygen depletion at the microscale. Therefore, we tested the hypothesis that sinking zooplankton carcasses are microsites of anaerobic nitrogen cycling that contribute to pelagic fixed-nitrogen loss even in the presence of ambient oxygen. Incubation experiments were performed with the ubiquitous copepods *Eudiaptomus* sp. and *Megacyclops gigas* at different ambient oxygen levels that sinking carcasses encounter during their descent in stratified lakes. ^{15}N-stable-isotope incubations revealed intense carcass-associated anaerobic nitrogen cycling only at low ambient oxygen levels (<25% air saturation). Dissimilatory nitrate reduction to ammonium (DNRA) dominated over denitrification and thus the potential for fixed-nitrogen loss was low. Consistent with this partitioning of anaerobic nitrogen cycling, the relative abundance of the carcass-associated marker gene for DNRA (*nrfA*) was ~20–400 times higher than that for denitrification (*nirS*). Additionally, the relative *nrfA* and *nirS* abundances were ~90–180 times higher on copepod carcasses than in lake water. This functional distinctiveness of carcass-associated bacterial communities was further substantiated by 16S rDNA-based fingerprinting. We conclude that the unique bacterial communities and microenvironments provided by zooplankton carcasses influence pelagic nitrogen cycling in lakes, but mainly at seasonally low ambient O_2 levels in the bottom water.

Keywords: copepods; nitrogen cycle; oxygen; ^{15}N-stable-isotope labeling; functional gene analysis; molecular community fingerprinting

Received: 28 May 2018; **Accepted:** 26 July 2018

INTRODUCTION

Mesozooplankton can be abundant in aquatic ecosystems including lakes and reservoirs, often amounting to several specimens per liter (Dubovskaya *et al.* 2003; Bickel, Tang and Grossart 2009; Tang *et al.* 2014; Tian *et al.* 2016). The dominant taxonomic groups of lake zooplankton are crustacean copepods and cladocerans (Bickel, Tang and Grossart 2009). Both the exoskeleton and the gut of live zooplankters are densely colonized with prokaryotes (Tang, Turk and Grossart 2010). Zooplankters are therefore perceived as pelagic 'microbial hot spots' that host prokaryotic communities that differ in composition from the free-living communities in the surrounding water (Moisander, Sexton and Daley 2015; Shoemaker and Moisander 2015). Due to high microbial activity and O_2 diffusion limitation, anoxic conditions can develop in the gut of live zooplankton, especially after food uptake (Tang *et al.* 2011). Accordingly, microbial N_2-fixation, a process that requires the absence of O_2, has been shown to be directly associated with live zooplankton (Zehr, Mellon and Zani 1998; Scavotto *et al.* 2015).

In lakes and other aquatic exosystems, up to 40% of the zooplankton community is found to be dead (Bickel, Tang and Grossart 2009; Elliott and Tang 2009; Tang *et al.* 2014). These zooplankton carcasses are rapidly colonized and degraded by bacteria (Tang, Hutalle and Grossart 2006; Bickel and Tang 2010) because the zooplankton cell tissue is particularly rich in proteins and hence in labile organic carbon and nitrogen (Tang *et al.* 2014). The intense microbial activities driving these degradation processes facilitate the development of hypoxic to anoxic conditions and the occurrence of anaerobic microbial processes inside zooplankton carcasses. Indeed, anoxic conditions develop in carcasses of large marine copepods (Glud *et al.* 2015) and anaerobic microbial nitrogen cycle (N-cycle) pathways, such as denitrification, were detected in the carcasses of marine copepods and ostracods (Glud *et al.* 2015; Stief *et al.* 2017).

Anaerobic N-cycling in pelagic microbial hot spots has previously been observed in sinking algae aggregates, especially when exposed to low-oxygen conditions (Klawonn *et al.* 2015; Ploug and Bergkvist 2015; Kamp *et al.* 2016; Stief *et al.* 2016). Anaerobic N-cycling comprises different pathways of dissimilatory nitrate reduction: In dissimilatory nitrate reduction to nitrite (DNRN) and dissimilatory nitrate reduction to ammonium (DNRA), fixed nitrogen is retained as dissolved inorganic nitrogen (DIN). Alternatively, fixed nitrogen is removed as N_2 gas via denitrification or anammox (Thamdrup 2012). Denitrification, DNRN and DNRA are quantitatively important anaerobic N-cycling pathways in sinking diatom aggregates (Kamp *et al.* 2016; Stief *et al.* 2016; Lundgaard *et al.* 2017). In contrast, anammox activity has so far not been detected, probably owing to the short-lived nature of sinking aggregates and the low growth rates of anammox bacteria. Denitrification activity has only recently been documented in carcasses of the large marine copepod *Calanus finmarchicus* (Glud *et al.* 2015). In the same study, the marker gene for denitrification *nirS*, encoding the cytochrome cd_1 nitrite reductase, was expressed in all carcasses, but only sporadically in living specimens. This indicates a higher potential for anaerobic N-cycling upon death of zooplankton when O_2 concentrations are reduced by high microbial respiration rates. In small marine zooplankton from an oxygen-depleted coastal basin, DNRA and denitrification were the most active pathways of anaerobic N-cycling, whereas anammox was the dominant pathway in the ambient anoxic seawater (Stief *et al.* 2017). This finding underlines that N-cycling associated with sinking carcasses can significantly differ from N-cycling in the surrounding water, probably owing to distinctive microbial communities that colonize and develop on zooplankton carcasses.

Pelagic hypoxia or even anoxia often occurs in freshwater lakes and reservoirs (Sand-Jensen and Lindegaard 2004). Highly eutrophic shallow lakes display diurnal variations of the ambient O_2 level, with high and low O_2 concentrations prevailing during day and night time, respectively (Sand-Jensen and Lindegaard 2004; Xu and Xu 2015). Deeper lakes are often temperature stratified during the summer, which in eutrophic and dystrophic lakes may lead to the development of hypoxic or anoxic conditions in the hypolimnion throughout the season (Gorham and Boyce 1989; Sand-Jensen and Lindegaard 2004). Sinking zooplankton carcasses may thus experience pronounced changes in ambient O_2 levels during their descent from the often oxygen-supersaturated epilimnion to the increasingly oxygen-depleted hypolimnion. Additionally, lake stratification leads to accumulation of copepod carcasses and other particles at the thermocline (Dubovskaya *et al.* 2003; Tang *et al.* 2014), a region often depleted in O_2. Therefore, sinking carcasses may remain in the hypoxic or anoxic water column for several days (Kirillin, Grossart and Tang 2012) and support intense organic matter degradation (Bickel and Tang 2010) and anaerobic N-cycling.

Here, we investigate the anaerobic N-cycling associated with sinking carcasses of the small copepods *Eudiaptomus gracilis* and *E. graciloides* and the large copepod *Megacyclops gigas* collected from two lakes in NE Germany contrasting in their trophy and hence their vertical O_2 distribution. The carcasses were incubated at ambient O_2 levels ranging from 0% to 100% air saturation to which carcasses are exposed when they sink through the water column of stratified lakes with an anoxic hypolimnion. Our first hypothesis was that zooplankton carcasses host anoxic microenvironments that allow anaerobic N-cycling even in an oxygenated macroenvironment. Our second hypothesis was that the rates of carcass-associated anaerobic N-cycling increase when ambient O_2 levels decrease. Carcass-associated anaerobic N-cycling was qualitatively and quantitatively analyzed in ^{15}N-stable-isotope incubations and by molecular analysis of the nitrite reductase genes involved in denitrification (*nirS*) and DNRA (*nrfA*). The distinctiveness of carcass-associated bacterial communities was assessed by 16S rDNA-based community fingerprinting of both bacteria on the carcasses and in the ambient water.

MATERIALS AND METHODS

Study site and organisms

Lake Dagow (53°09'01'N, 13°03'60'E) and Lake Stechlin (53°09'03'N, 13°01'40'E) are located in NE Germany and are connected via a small outflow. Lake Dagow is a shallow (9 m), eutrophic lake that experiences seasonal hypoxia, with the bottom water falling anoxic below a depth of 6 m every year. Lake Stechlin is a deep (69.5 m), oligotrophic lake with no anoxia or hypoxia even at 50 m depth. Three different species of zooplankton that were abundant in any of these two lakes at the time of this study (September 2015) were investigated in laboratory experiments: The small (prosome length 0.5–0.8 mm), omnivorous copepods *Eudiaptomus gracilis* and *E. graciloides* from Lake Dagow (Brandl 2005; Šorf and Brandl 2012) and the large (prosome length 2.5–3.0 mm), carnivorous copepod *Megacyclops gigas* from Lake Stechlin (Brandl 2005).

Sample collection

Eudiaptomus sp. were collected in Lake Dagow just below the water surface by horizontal net tows with a plankton net of 250 μm mesh size and 0.5 m mouth size and carefully transferred to 1-L glass bottles. The net was rinsed between each tow to remove zooplankton carcasses. Surface lake water was collected in 5-L canisters and filtered through 5-μm polycarbonate membranes. *Megacyclops gigas* was collected in Lake Stechlin at 10–15 m water depth by deploying sediment traps and leaving them in the water for 3 days. Living *M. gigas* were abundant in the traps, presumably taking advantage of accumulated food. *Megacyclops gigas* was kept in darkness at 20°C in 90-μm filtered, oxygenated surface water from Lake Stechlin. For feeding, mixed zooplankton from Lake Stechlin was added to the storage tank containing *M. gigas*.

Preparation of copepod carcasses

When returning to the laboratory, *Eudiaptomus gracilis* and *E. graciloides* were isolated from the Lake Dagow zooplankton samples, carefully excluding the bottom layer in the collection bottle to avoid transferring already dead specimens. The pooled *Eudiaptomus* sp. were then exposed to 10% acetic acid for a few seconds followed by several immersions in sterile-filtered Lake Dagow water to get rid of residual acid. The *Eudiaptomus* sp. carcasses were then transferred to beakers with Lake Dagow water collected on the same day. The beakers were put on a shaker table set at slow speed and left in darkness at 20°C overnight, to allow for colonization by the free-living microbial community in the lake water. *Megacyclops gigas* specimens were killed and preincubated on the day before the incubation experiments by the same procedure.

Experimental schedule

Short-term $^{15}NO_3^-$-incubation experiments were performed with and without copepod carcasses as summarized in Table 1. For *Eudiaptomus* sp., four incubation experiments with three replicates each were designated $E1_{low}$, $E1_{high}$, $E2_{low}$ and $E2_{high}$ in accordance with the different targeted ambient O_2 levels. For *M. gigas*, four incubation experiments with five replicates each were designated $M1a_{low}$, $M1b_{low}$, $M2_{low}$, and $M2_{high}$. Note that for incubation experiment $M1a_{low}$, the copepods were killed just prior to the short-term incubation experiments, whereas for all remaining experiments, the prepared carcasses were preincubated overnight (see previous section). For controls without copepod carcasses, three incubation experiments with five replicates each were designated Ctr_{low}, $Ctr_{intermediate}$, and Ctr_{high}, in accordance with the different targeted ambient O_2 levels of 0%, 20% and 100% air saturation.

Experimental procedure

Oxygen dynamics and anaerobic N-cycling were studied in short-term incubation experiments. Prior to the incubations, 100 *Eudiaptomus* sp. or 40 *M. gigas* carcasses each were transferred to replicate 30-mL glass bottles. Despite this larger number of *Eudiaptomus* sp. carcasses, the total biomass was still ca. six times higher in *M. gigas* incubations. The bottles were equipped with oxygen-sensitive optode patches (SensorSpot, PyroScience, Aachen, Germany) fixed to the inner side of the bottle wall and interrogated from the outside by a FireSting O_2 meter (PyroScience, Aachen, Germany). For reasons of conformity regarding water chemistry and free-living bacterial community, all *Eudiaptomus* sp., *M. gigas*, and control incubation experiments were made with 5-μm-filtered Lake Dagow water. The lake water was amended with $^{15}NO_3^-$ (98 atom% ^{15}N, Sigma-Aldrich, U.S.A.) to a final concentration of 5 μM. The background concentration of NO_3^- in Lake Dagow water was 1.3 μM. The ambient O_2 level was adjusted by flushing the lake water with O_2 and He using a thermal mass flow controller (Brooks Instrument, Hatfield, USA). The bottles were closed and sealed with gas-tight rubber stoppers without entrapping gas bubbles and then incubated on a plankton wheel in darkness at 20°C. After 0, 1.5, 3, 4.5 and 6 h, the O_2 concentration was measured and a water sample (3 mL) was taken from each bottle through the rubber stopper. At each sampling time point, the water withdrawn from the bottle was replaced with $^{15}NO_3^-$-enriched lake water that had been adjusted to an O_2 concentration that roughly would compensate for the drop in O_2 concentration since the last sampling time point (Stief *et al.* 2016). The 3-mL water sample was split into two samples: (i) 1.5 mL was transferred to a 3-mL He-flushed, half-evacuated exetainer (Labco, Wycombe, UK) containing 50 μL $ZnCl_2$ (50% w/v) that was stored at room temperature for later ^{15}N-analyses and (ii) 1.5 mL was transferred to a 2-mL sample tube that was stored at –20°C for later DIN analysis.

Nitrogen analyses

Samples for DIN analysis (NO_3^-, NO_2^- and NH_4^+) were filtered through 0.22-μm membranes prior to analysis. Nitrate plus nitrite concentrations were measured on an NO_x analyzer (42 C, Thermo Fisher Scientific) with the VCl_3 reduction assay (Braman and Hendrix 1989). Nitrite was quantified via the Griess reaction using a spectrophotometer (Multiskan GO Microplate Spectrophotometer, Thermo Fisher Scientific) after Garcia-Robledo, Corzo and Papaspyrou (2014). Ammonium was analyzed after Holmes *et al.* (1999) on a Turner Trilogy Fluorometer (Model 7200-041, Turner Design). The isotopically labeled nitrogen species ^{15}N-N_2 ($^{29}N_2$ + $^{30}N_2$), $^{15}NO_2^-$, and $^{15}NH_4^+$ were analyzed on a gas chromatography-isotopic ratio mass spectrometer (GC-IRMS; Thermo Delta V Plus, Thermo Fisher Scientific) (Dalsgaard *et al.* 2012). A subset of the samples was analyzed for N_2O on a gas chromatograph (GC 7890, Agilent Technologies). The samples for $^{15}N_2$ and N_2O analysis were withdrawn from the headspace of the 3-mL exetainers, after which ^{15}N-labeled NO_2^- and NH_4^+ were analyzed with the sulfamic acid and the hypobromite assay, respectively (Warembourg 1993; McIlvin and Altabet 2005). The efficiency of these chemical conversion steps was verified with $^{15}NO_2^-$ and $^{15}NH_4^+$ calibration standards ranging between 0 and 5 μM in concentration.

Rate calculations and statistics

Oxygen consumption and N-turnover rates were calculated from linear regressions of the concentration time series, accounting for any dilution during the sampling process. Production rates of total NH_4^+ from DNRA, total NO_2^- from DNRN and total N_2 from denitrification were calculated from production rates of $^{15}NH_4^+$, $^{15}NO_2^-$ and $^{15}N_2$, respectively, and the initial $^{15}NO_3^-$-labeling fraction in the lake water (i.e. 0.79) to account for the $^{14}NO_3^-$ present in the water. Since the N-turnover rates measured in carcass incubations included any activity from the free-living microbial community in the 5-μm-filtered lake water, the N-turnover rates measured in the respective control incubations without carcasses were subtracted to approximate the carcass-associated N-turnover rates. In incubations in which

Table 1. Overview of incubation experiments in $^{15}NO_3^-$-enriched lake water.

Copepod taxon	Name of experiment	Incubation temp. (°C)	Ambient O_2 level* (% AS)	No. of replicates	Day of copepod collection	Day of incubation experiment	Duration of preincubation (h)
Eudiaptomus sp. from Lake Dagow (0–1 m)	$E1_{low}$	20	9.4 ± 1.5	3	7.9.15	8.9.15	16
	$E1_{high}$	20	54.3 ± 1.0	3	7.9.15	8.9.15	16
	$E2_{low}$	20	8.2 ± 3.0	3	11.9.15	12.9.15	16
	$E2_{high}$	20	86.3 ± 8.4	3	11.9.15	12.9.15	16
Megacyclops gigas from Lake Stechlin (10–15 m)	$M1a_{low}$	20	3.7 ± 1.5	5	22.9.15	24.9.15	<1
	$M1b_{low}$ **	20	1.4 ± 1.2	5	22.9.15	24.9.15	16
	$M2_{low}$ **	20	7.5 ± 5.8	5	22.9.15	25.9.15	16
	$M2_{high}$	20	75.1 ± 16.5	5	22.9.15	25.9.15	16
Control (incubations without carcasses)	Ctr_{low}	20	4.0 ± 1.1	5	n.a.	24.9.15	n.a.
	$Ctr_{intermediate}$	20	20.5 ± 1.6	5	n.a.	25.9.15	n.a.
	Ctr_{high}	20	95.3 ± 6.4	5	n.a.	25.9.15	n.a.

*Ambient air saturation (AS) levels of O_2 are given as means ± SD (n = 3–5).
**Anoxic conditions were reached in some of the replicate incubation bottles. n.a. = not applicable.

unintended anoxic events occurred (i.e. $M1b_{low}$ and $M2_{low}$), the N-turnover rates were additionally calculated for the hypoxic and anoxic phase separately.

The slope of the regression lines and the mean slopes were analyzed with t-tests to identify rates that were significantly different from zero. The effect of the ambient O_2 level on the turnover rates of O_2, NO_3^-, NO_2^-, NH_4^+, and process rates of DNRN, DNRA, and denitrification in *Eudiaptomus* sp. or *M. gigas* incubations was tested with ANOVA (one-way), followed by the Tukey post-hoc test. The effect of overnight preincubation on N-turnover rates was analyzed with t-tests. The effect of (i) ambient O_2 level and day of copepod collection in *Eudiaptomus* sp. or *M. gigas* carcass incubations and of (ii) ambient O_2 level and copepod taxon in the whole sample set was tested with ANOVA (two-way, two-factorial, without interaction), followed by the Tukey post-hoc test on the same variables as above. ANOVA and post-hoc tests were performed in R (R core team, Version 3.2.4).

Bacterial community fingerprinting

To separate the carcasses from the water after the incubations were completed, the content of each incubation bottle was filtered onto 5.0-μm Nuclepore polycarbonate membranes. Membranes were immediately frozen in liquid nitrogen and stored at –80°C until further processing. Biomass from Lake Dagow and Lake Stechlin water was sampled on the day of copepod collection by filtration through 0.22-μm Nuclepore polycarbonate membranes, which were stored like the carcass samples.

DNA from carcasses was extracted with a protocol modified from Nercessian *et al.* (2005) using chloroform-phenol-isoamyl and zirconium beads with the addition of potassium phosphate buffer. For DNA extractions from water samples, the PowerWater DNA Isolation kit (MO BIO, Carlsbad, USA) was used following the manufacturer's protocol. DNA was quantified with a fluorometer using the Quant-iT Picogreen kit (Invitrogen, Carlsbad, USA), providing average yields of 6.9, 84.5 and 122.2 ng μL^{-1} from 100 *Eudiaptomus* sp. carcasses, 40 *M. gigas* carcasses, and ~750 mL lake water, respectively.

For terminal restriction fragment length polymorphism (T-RFLP) analysis (Avaniss-Aghajani *et al.* 1994; Liu *et al.* 1997) of the bacterial community, the 16S rRNA genes were amplified by PCR using the phosphoramidite fluorochrome 5-carboxyfluorescein labeled, Bacteria-specific forward primer B27FAM (50-AGRGTTYGATYMTGGCTCAG-30) and the reverse primer U519R (50-GWATTACCGCGGCKGCTG-30). PCR was performed in 50-μL reactions with final amounts of 5–10 ng template, 20 pmol of each primer, 10 nmol dNTPs in equal amounts, 5 μL 10x Taq-buffer with $(NH_4)_2SO_4$, 1.25 units Taq-polymerase and 125 nmol $MgCl_2$ (all: Thermo Fisher Scientific). Denaturation at 94°C for 2 min was followed by 32 cycles of 94°C for 20 s, 54°C for 45 s, and 72°C for 45 s, with a final elongation step at 72°C for 5 min. Successful amplification was verified by agarose gel (1.5%) electrophoresis. The ~500 base pair (bp) PCR product was incubated with 5 U of *Bsu*RI in buffer R (Thermo Fisher Scientific) at 37°C for 12 hr followed by heat inactivation at 80°C for 20 min. The resulting restriction fragments were purified with the GeneJET PCR purification kit (Thermo Fisher Scientific) and ~100 ng were sent for fragment length analysis to Uppsala Genome Center (Sweden).

For the analysis of the T-RFLP data, initial fragment sizing was carried out with the software Peak Scanner (Applied Biosystems, Foster City, USA). Noise filtration (factor 1.2 based on peak area), clustering (factor 0.5) and construction of data matrices were performed with the online program T-RFLP analysis EXpedited (http://trex.biohpc.org/). The operational taxonomic unit (OTU) fluorescence was standardized to the total fluorescence of all OTUs in a sample, and matrices of different sample combinations of interest were created including only OTUs present in more than one sample and with a relative abundance of >0.5%. Data matrices were analyzed with R (R core team, version 3.2.4) and the R-package vegan (Oksanen *et al.* 2013), where the dissimilarities between samples and their respective OTUs were calculated and visualized with non-metric multidimensional scaling (NMDS). The function metaMDS was used to find the best fit between Bray–Curtis dissimilarities and ordinations with minimal stress (goodness of fit). The data values were submitted to Wisconsin double standardization. The function found species scores as weighted averages of site scores, but expanded them so that species and site scores had equal variances (Oksanen *et al.* 2013). All NMDS settled for two dimensions and low stress ranging from 0.086 to 0.112.

Bacterial functional marker gene abundances

The bacterial and archaeal 16S rRNA genes as well as the functional marker genes *nirS* (denitrification) and *nrfA* (DNRA) were quantified by quantitative PCR (qPCR) in duplicate 25-μL reactions with 5–10 ng template, 25 pmol of each of the respective primers (Table S1, Supporting Information), RealQ Plus 2 × Master Mix (Ampliqon) and 10 μg bovine serum albumin (BSA; final conc. 4 μg μL^{-1}) using a CFX Connect Real-time System (BIO-RAD). Amplification was started with a denaturing step at 95°C for 15 min followed by 40 (16S, *nirS*) or 32 (*nrfA*) cycles of denaturing at 95°C for 20 s, annealing for 30 s at primer-specific temperatures (Table S1, Supporting Information) and extension at 72°C for 30 s (16S, *nirS*) or 45 s (*nrfA*). The products were analyzed by melting curves from 65°C to 95°C in steps of 0.5°C with 5 s at each step. Standard curves were made from serial 10-fold dilutions of the target genes (10^1–10^7 copies per μL).

Diversity of *nrfA* in copepod carcasses

To assess the diversity of *nrfA*, the gene was amplified from copepod carcass samples (*M. gigas*) by PCR with the corresponding primers (Table S1, Supporting Information). The PCR-product was cloned into the plasmid vector (pCR 4-TOPO) using the TOPO TA Cloning Kit for sequencing (Invitrogen) and One Shot TOP10 Chemical competent *E. coli* cells were transformed with the ligated plasmids following the manufacturer's instructions. The inserts from 60 clones were amplified by colony PCR using M13 primers and the PCR products were sent for sequence analysis to the Institute of Clinical Molecular Biology (IKMB), Kiel University. Fifty-four clones returned high-quality sequences from which the vector sequences were trimmed off. The resulting, around 237 bp long DNA sequences were translated and phylogenetically analyzed using the *NrfA* alignment from Welsh *et al.* (2014) in the software package ARB (Ludwig *et al.* 2004). The sequences have been deposited at Genbank under the accession numbers MG806931-MG806984.

Preparation of *nrfA* standard for qPCR

In order to be used as standards in the qPCR, two *nrfA* clones were chosen, grown in LB medium (Miller) with 50 μg mL^{-1} kanamycin overnight at 37°C and the plasmids extracted with the GeneJet Plasmid Miniprep kit (Thermo Fisher Scientific). The *nrfA* gene fragment was amplified with PCR as described above and the DNA concentration of the PCR product was quantified with a Quant-iT Picogreen dsDNA Assay Kit (Molecular Probes by Life Technologies) using a Victor2 1420 Multilabel Counter (Wallac). With this information, the gene copy number was calculated and dilution series of 10^1 to 10^7 copies were prepared.

RESULTS

Oxygen dynamics

In most experiments, ambient O_2 levels remained relatively stable throughout the incubation (Fig. S1, Supporting Information), in particular during the *Eudiaptomus* sp. carcass incubations and the control incubations without any carcasses (Fig. S1A and C, Supporting Information). During some of the incubations with the much larger *M. gigas* carcasses, however, strong O_2 consumption caused pronounced drops in the ambient O_2 level (Fig. S1B, Supporting Information). In $M1b_{low}$ and $M2_{low}$, this led to the occurrence of anoxic events in the majority of the replicates, already after 3 h of incubation. In $M2_{low}$, the re-injection of oxygenated water during water sampling made the ambient O_2 level fluctuate between 0% and ~10% air saturation. To account for these anoxic events, carcass-associated anaerobic N-cycling was not only evaluated for the total incubation period, but also separately for the hypoxic and anoxic phases that occurred in $M1b_{low}$ and $M2_{low}$ (see below).

Carcass degradation

The carcass-associated O_2 consumption and NH_4^+ production was used to assess the rate of microbial degradation of the carcass biomass. Oxygen concentration time series were re-constructed from the concentration decreases measured between consecutive sampling time points, while NH_4^+ concentration time series were measured directly (Fig. 1A and B). Across all experiments, the O_2 consumption and NH_4^+ production rates calculated from the concentration time series were significantly, linearly correlated ($R^2 = 0.894$, $P < 0.001$) (Fig. 1C). Assuming a respiratory quotient of 1.0 during carcass degradation, the O_2 consumption rates are numerically equivalent with CO_2 production rates. The slope of the regression line in Fig. 1C then corresponds to an average C/N ratio of 6.0 between the CO_2 and NH_4^+ produced during carcass degradation. This C/N ratio was mainly carried by the higher O_2 consumption and NH_4^+ production rates during incubation of the large *M. gigas* carcasses compared to the much smaller *Eudiaptomus* sp. carcasses (Fig. 1C; Table S2, Supporting Information). It needs to be noted that for the two incubation series in which anoxic events occurred (i.e. $M1b_{low}$ and $M2_{low}$), the re-constructed O_2 concentration time series underestimate the actual rate of CO_2 production that may partially be due to anaerobic respiration processes, such as dissimilatory NO_3^- reduction or SO_4^{2-} reduction.

Within each copepod taxon and O_2 treatment, sample history had a strong effect on carcass degradation, i.e. the E2- and M2-incubation series showed several times higher rates than the corresponding E1- and M1-incubation series. Furthermore, carcass degradation was stimulated by the high ambient O_2 levels in $E1_{high}$ and $E2_{high}$ (but not in $M2_{high}$) and by the overnight preincubation in $M1b_{low}$ (Table S2, Supporting Information).

Nitrogen cycling

Consistent temporal changes in NO_3^- concentration indicative of net NO_3^- production or consumption were rare (Fig. 2A and B). A pronounced decrease in NO_3^- concentration was only observed in the low-oxygen experiment $M2_{low}$ (Fig. 2B). Notably, this decrease in NO_3^- concentration only started when the first anoxic event occurred. The strongest increases in NO_2^- and NH_4^+ concentration due to DNRN and DNRA activity, respectively, were likewise observed in the low-oxygen experiments $E2_{low}$, $M1b_{low}$ and $M2_{low}$ (Fig. 2C–F). The onset of anoxic events in $M1b_{low}$ and $M2_{low}$ further accelerated the increase in NO_2^- and NH_4^+ concentration. In contrast, rather weak increases in N_2 concentration due to denitrification activity were observed in all experiments, and anoxic events did not trigger stronger increases in N_2 concentration (Fig. 2G and H). Consistent temporal changes in N_2O concentration were not observed in any of the experiments (data not shown).

General trends for the rates of carcass-associated anaerobic N-cycling were that (i) DNRA and DNRN showed higher rates than denitrification, (ii) the larger *M. gigas* carcasses hosted higher carcass-specific rates than the smaller *Eudiaptomus* sp. carcasses, and (iii) anaerobic N-cycling was more intense at low

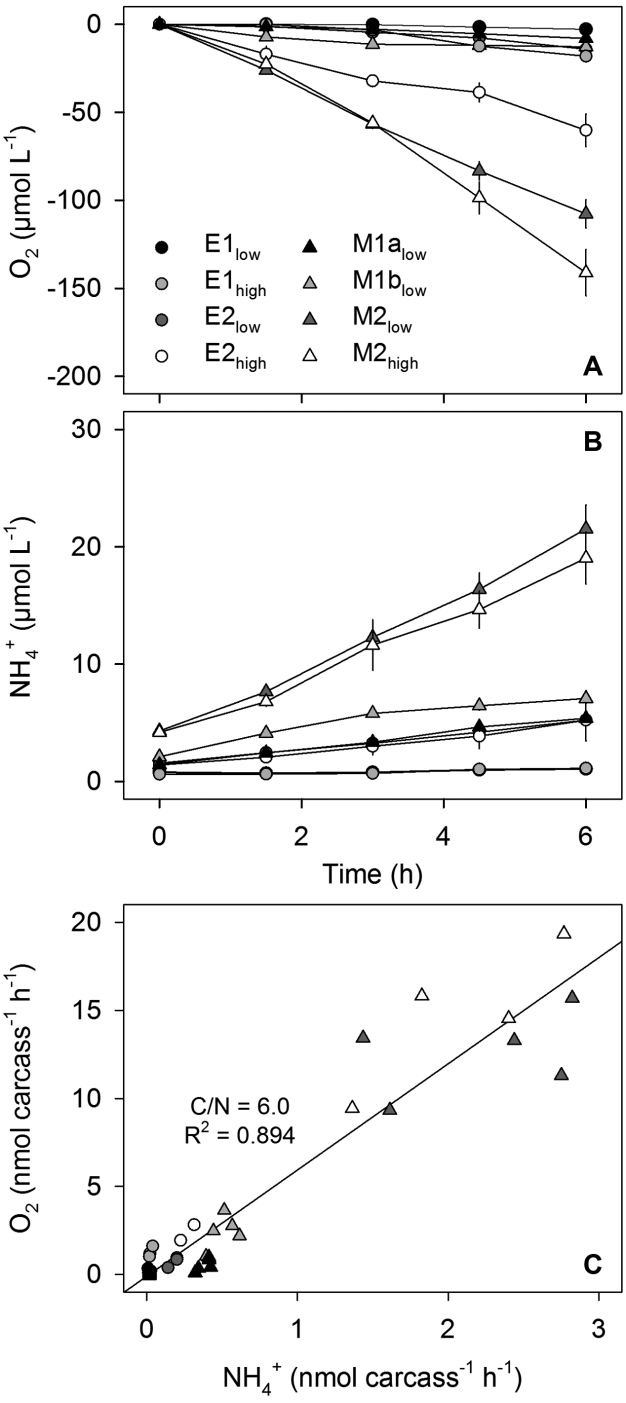

Figure 1. (**A**) Re-constructed O_2 and (**B**) measured NH_4^+ concentration time series in *Eudiaptomus* sp. and *M. gigas* incubation experiments. Re-constructed O_2 concentration time series were obtained by summing up the decreases in O_2 concentration measured between consecutive sampling time points. (**C**) Correlation between O_2 consumption and NH_4^+ production rate calculated for all *Eudiaptomus* sp. and *M. gigas* incubation experiments. With a respiratory quotient of 1.0, the O_2 consumption rate is equal to the CO_2 production rate, and then the slope of the regression line corresponds to the overall C/N ratio of carcass degradation. Note that the total carcass biomass was ca. 6-fold larger in *Eudiaptomus* sp. than in *M. gigas* incubations. In (**A**) and (**B**), means ± SE (n = 3–5) are shown.

ambient O_2 levels (Fig. 3; Tables S2–S4, Supporting Information). Additionally, the only significant correlation between rates of the three anaerobic N-cycle pathways was observed between DNRA and DNRN ($R^2 = 0.514$, $P < 0.0001$, n = 30). Rates of DNRA, DNRN and denitrification were significantly different from zero in most, but not all of the low-oxygen experiments (Table S2, Supporting Information). In contrast, rates of these anaerobic N-pathways were not significantly different from zero in the high-oxygen experiments, except the significant DNRN rate in $M2_{high}$. Consequently, the ambient O_2 level had in most cases a statistically significant effect on the rates of carcass-associated anaerobic N-pathways (Table S4, Supporting Information). This regulatory role of the ambient O_2 level was further substantiated in the two low-oxygen experiments $M1b_{low}$ and $M2_{low}$ in which anoxic events occurred repeatedly. The rates of DNRA (in $M2_{low}$) and DNRN (in $M1b_{low}$ and $M2_{low}$), but not denitrification, increased significantly following the onset of anoxic events (Student's t-test: $P < 0.05$).

The rates of carcass-associated anaerobic N-pathways were also influenced by sample history and sample treatment. The day of copepod collection in the lake had a significant effect on DNRA and DNRN rates in each of the two *Eudiaptomus* sp. incubation series and on DNRA, DNRN and denitrification rates in each of the two *M. gigas* incubation series (Table S4, Supporting Information). Additionally, the overnight preincubation of carcasses in $M1b_{low}$ increased the rates of NO_3^- consumption and DNRN, but not DNRA and denitrification, significantly (Student's t-test: $P < 0.05$).

Bacterial community composition

Using *Bsu*RI, 134 OTUs were detected in the complete sample set. Table S5 (Supporting Information) shows how many OTUs were associated with copepods in each of the different incubation experiments and how many were present in the *in situ* water of the two lakes. When subjected to non-metric two-dimensional scaling, the carcass-associated bacterial communities of *Eudiaptomus* sp. and *M. gigas* clustered separately, as did the free-living communities from Lake Dagow and Lake Stechlin (Fig. 4A), indicating that both copepod taxon and lake type drove composition of the total bacterial communities. The carcass-associated communities further clustered into four groups according to day of copepod collection, but not into high- and low-oxygen incubations (Fig. 4B), indicating that sample history was more important for shaping the total bacterial communities than the short-term exposure to different O_2 levels. $M1a_{low}$ and $M1b_{low}$ communities were dissimilar (despite the same day of copepod collection), indicating that the carcass-associated bacterial community changed during the overnight preincubation (Fig. 4B).

Bacterial gene abundance

The abundance of carcass-associated bacterial 16S rRNA genes varied between 3.8×10^6 and 1.6×10^8 per carcass (Fig. 5A). Across all experiments, 16S rDNA abundance was significantly correlated with the carcass-specific O_2 consumption rate (Spearman: $R^2 = 0.627$, $P < 0.001$). The relative abundance of carcass-associated *nrfA* genes varied between 9.9×10^{-3} and 4.2×10^{-1} per 16S rDNA copy and was 90 ± 20 times higher than in lake water (Mean ± SE, n = 29) (Fig. 5B). The relative *nrfA* abundance was significantly, linearly correlated with the carcass-specific DNRA rate ($R^2 = 0.168$, $P = 0.034$) and O_2 consumption rate ($R^2 = 0.769$, $P < 0.001$). The relative abundance of carcass-associated *nirS* genes varied between 5.4×10^{-4} and 8.1×10^{-3} per 16S rDNA

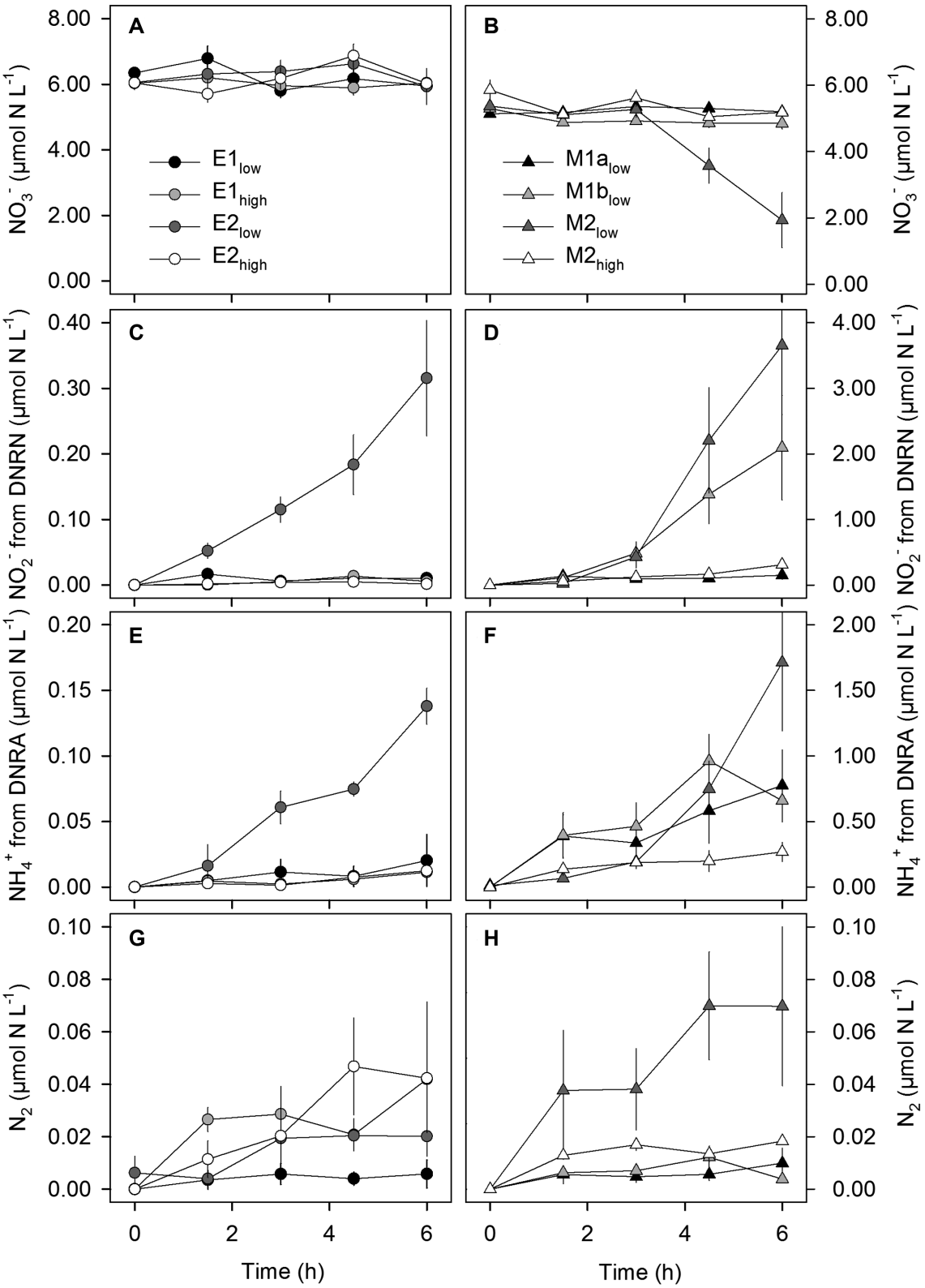

Figure 2. Concentration time series of (**A** and **B**) NO_3^-, (**C** and **D**) NO_2^- from DNRN, (**E** and **F**) NH_4^+ from DNRA, and (**G** and **H**) N_2 from denitrification as measured in *Eudiaptomus* sp. and *M. gigas* incubation experiments. Note different scales of y-axes between *Eudiaptomus* sp. and *M. gigas* incubation experiments in panels (**C–F**). Note also that the total carcass biomass was ca. 6-fold larger in *Eudiaptomus* sp. than in *M. gigas* incubations. Means ± SE (n = 3–5) are shown.

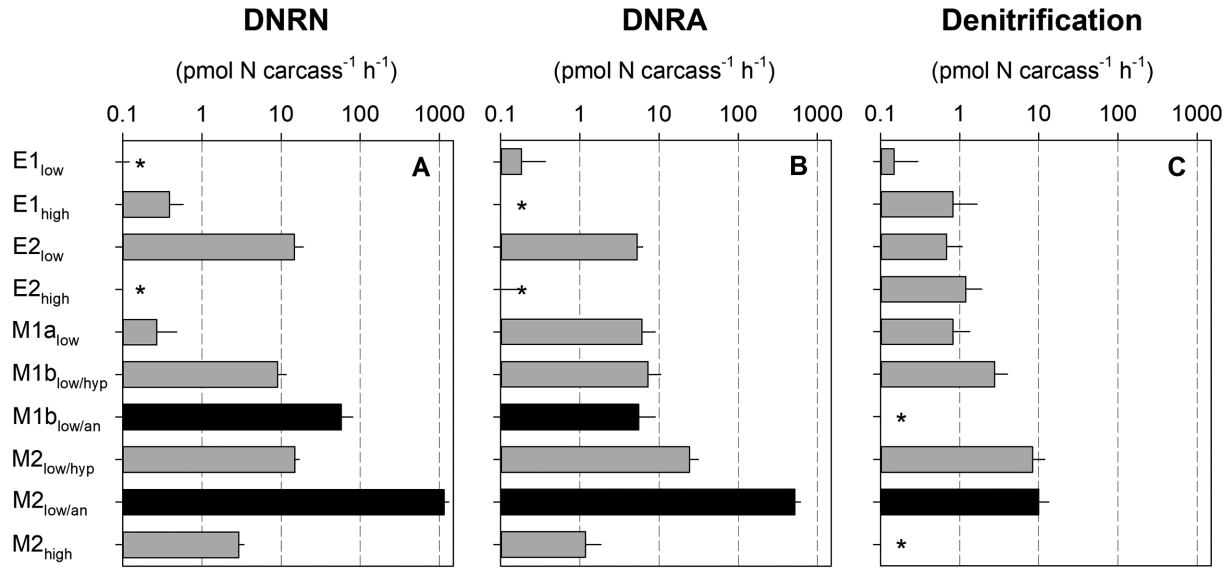

Figure 3. Carcass-specific rates of (**A**) DNRN, (**B**) DNRA and (**C**) denitrification calculated for the *Eudiaptomus* sp. and *M. gigas* incubation experiments. For $M1b_{low}$ and $M2_{low}$, rates are presented for the hypoxic (/hyp, grey bars) and anoxic (/an, black bars) phases that were observed during the incubation. Means ± SE (n = 3–5) are shown. Note logarithmic scale of the x-axis. Asterisks mark average rates <0.1 pmol N carcass^{-1} h^{-1}.

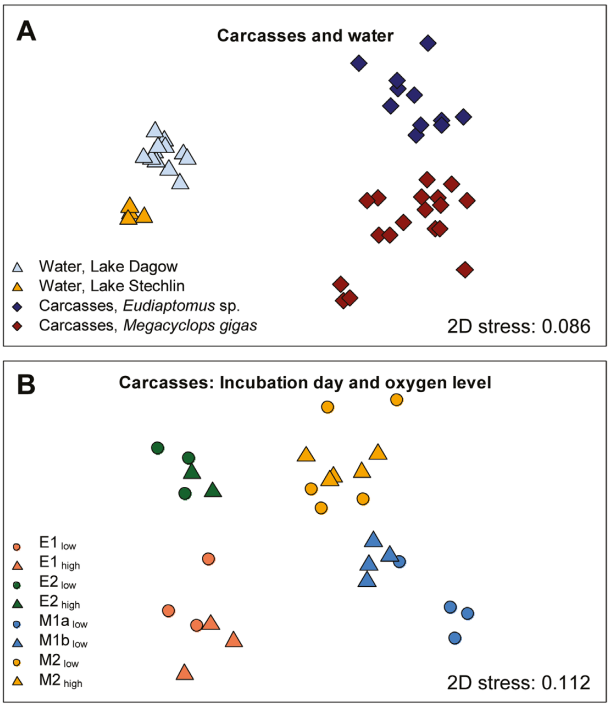

Figure 4. Multivariate statistical analysis of bacterial community composition based on T-RFLP community fingerprinting. The dissimilarities between (**A**) copepod taxa and origin of water and (**B**) the eight different carcass incubation experiments were analyzed with the Bray–Curtis index and plotted with NMDS. 2D stress values are shown within the plots. See *Materials and methods* section for details.

copy and was 178 ± 35 times higher than in lake water (Fig. 5C). The relative *nirS* abundance was negatively correlated with the carcass-specific denitrification rate ($R^2 = 0.355$, $P = 0.001$) and O_2 consumption rate ($R^2 = 0.389$, $P < 0.001$). Across all copepod taxa, the relative *nrfA* abundance was ~20–400 times higher than the relative *nirS* abundance. Archaea were, based on the quantification of their 16S rRNA gene, not present or extremely low in abundance in both lake water and on carcasses.

NrfA diversity

The 54 *NrfA* sequences retrieved clustered into 15 unique sequences, and phylogenetic analysis revealed their high similarity to sequences belonging to *NrfA* of clade A that has been defined by Welsh *et al.* (2014) (Fig. S2, Supporting Information). More specifically, they all fell into a sub-cluster of sequences originating from the *Aeromonas* species *A. veronii*, *A. salmonicida* subsp. *salmonicida*, and *A. caviae*, which show a relatively small phylogenetic distance to the other sequences of cluster A (Fig. S2, Supporting Information).

DISCUSSION

Pathways of carcass-associated anaerobic N-cycling

The dominant anaerobic N-cycle pathways associated with carcasses of both *Eudiaptomus* sp. and *Megacyclops gigas* were DNRA and the tightly correlated DNRN. In contrast, only very low rates of denitrification were measured and exclusively on the larger *M. gigas* carcasses. Anammox was ruled out as an important carcass-associated anaerobic N-cycle pathway because $^{30}N_2$ rather than $^{29}N_2$ was the main isotopic form of N_2 produced. Generally, only 1%–4% of the total dissolved ^{15}N-labeled compounds produced from the added $^{15}NO_3^-$ were in the form of N_2, which would contribute to pelagic fixed-nitrogen loss. The majority of ^{15}N-labeled compounds, however, were released as NH_4^+ and NO_2^- into the surrounding water where they can be used by free-living bacteria and microalgae for N-assimilation and nitrification. Consequently, our study on copepod carcassess revealed a rather low potential for a direct contribution to fixed-nitrogen loss at the ecosystem level.

Glud *et al.* (2015) studied denitrification in carcasses of the large marine copepod *Calanus finmarchicus* (prosome length ~2.6 mm) and measured carcass-specific N_2 production rates under

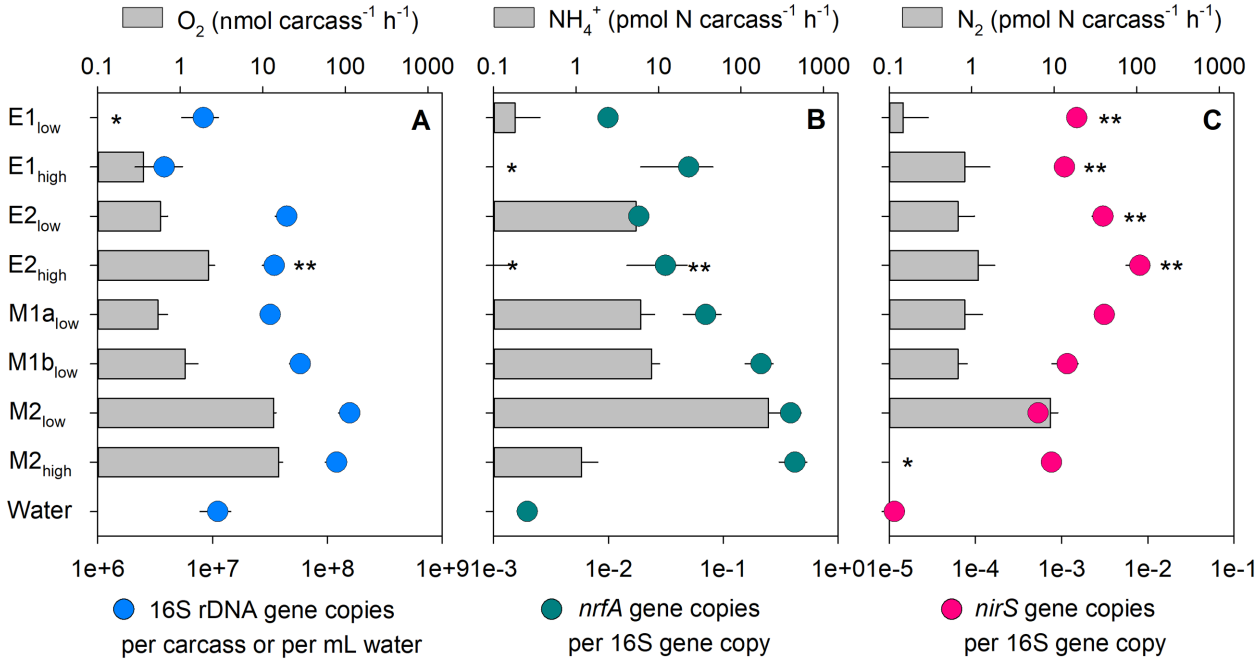

Figure 5. Copy numbers of carcass-associated (**A**) 16S rRNA genes (per carcass) and the nitrite reductase genes (**B**) *nrfA* and (**C**) *nirS* (per 16S rDNA gene copy) in relation to carcass-specific rates of O_2 consumption, NH_4^+ production, and N_2 production, respectively. Gene abundance of 16S rDNA (per mL lake water) and *nrfA* and *nirS* (per 16S rDNA gene copy) in lake water are shown for comparison. Means ± SE (n = 3–5) are shown. Note logarithmic scale of the two x-axes. Asterisks mark average rates <0.1 pmol N carcass^{-1} h^{-1}. Double asterisks mark gene copy numbers obtained in a single qPCR run; the remaining samples were run in duplicate.

anoxic conditions that were two orders of magnitude higher than the rates measured in the present study. Likewise, significantly higher denitrification rates were measured in relatively small copepod carcasses (prosome length ≤0.5 mm) from a tropical oxygen minimum zone (Stief *et al.* 2017). The unexpectedly high denitrification rates in the latter study might be explained by the use of $^{15}NO_2^-$ instead of $^{15}NO_3^-$, if DNRN was rate-limiting for carcass-associated denitrification. It might, however, also be a specific trait of the three studied lake copepod species that carcass-specific denitrification rates were lower than in all tested marine copepod species. For tropical marine copepods and ostracods, DNRA was also identified as an important carcass-associated N-pathway with rates ~10–25 times higher than denitrification rates under anoxic conditions (Stief *et al.* 2017).

Significant DNRN activities have also been reported for sinking algae aggregates and were explained by the lack of any NO_3^- limitation in the pelagic zone and inside the aggregates (Stief *et al.* 2016; Lundgaard *et al.* 2017). Similarly, NO_2^- production was observed in activated sludge in which NO_3^- diffused to the very center of the individual sludge flocs (Schramm *et al.* 1999). In contrast, diffusional NO_3^- limitation in sediments favors N_2 and NH_4^+ over NO_2^- production (Stief *et al.* 2010; Devol 2015). The carcasses from this study are not expected to have experienced such diffusional NO_3^- limitation because of their relatively small size and low NO_3^- consumption rates. The carcass-associated DNRN rates were significantly correlated with the DNRA rates, but not with the denitrification rates. Additionally, both DNRN and DNRA, but not denitrification, were boosted by the onset of anoxic conditions during incubation. Given these similarities, it might be speculated that the two pathways were mediated by the same microorganisms (i.e. DNRA bacteria) carrying out the sequential DNRA pathway either completely or partially. However, it cannot be excluded that true DNRN bacteria that do not possess the enzymes for NO_2^- reduction to NH_4^+ or N_2 were responding to the change in ambient O_2 levels in the same way and at similar rates as DNRA bacteria.

DNRA activities associated with the carcasses of the lake copepods studied here were in a similar range as reported for small marine copepods (Stief *et al.* 2017). The high relative importance of this N-cycle pathway on both freshwater and marine copepods is likely explained by the unique microenvironments and substrates that sinking zooplankton carcasses provide to DNRA bacteria. Anoxia and the copious supply of electron donors inside the gut of living copepods (Tang *et al.* 2011) may favor the growth and persistence of enteric bacteria many of which are capable of DNRA (Cole 1996; Tiso and Schechter 2015). Additionally, the exoskeleton of copepods is commonly colonized by *Vibrio* spp. that degrade chitinous compounds (Montanari *et al.* 1999; Tang, Turk and Grossart 2010; Shoemaker and Moisander 2015), and many *Vibrio* spp. and related bacterial genera possess the genes necessary for DNRA (Bonin 1996; Rusch and Gaidos 2013; Kraft *et al.* 2014).

The dominance of DNRA relative to denitrification was supported by the higher relative abundance of the functional marker gene *nrfA* than *nirS*. For the smaller *Eudiaptomus* sp. carcasses, *nrfA* was on average 18-fold more abundant than *nirS*, while the rates of DNRA were 8-fold higher than that of denitrification. For the larger *M. gigas* carcasses, however, *nrfA* was on average 462-fold more abundant than *nirS*, while the rates of DNRA were 40-fold higher than that of denitrification. The discrepancies between gene abundance and rates and between different zooplankton taxa hint to differences at the level of gene transcription and/or differences in the regulation of enzyme activities by microenvironmental conditions or substrate supply related to zooplankton taxon. The phylogenetic analysis of the *nrfA* sequences indicated a high specificity of the used primer set as only *nrfA* sequences were retrieved. On the nucleotide level, the most different clones were still 94.5% identical, indicating that either a fairly low diverse community of *nrfA*-containing

bacteria was present or that the primers did not amplify all *nrfA* genes. This suggests that the *nrfA* abundances determined by qPCR are rather under- than overestimates. Interestingly, the *nrfA* sequences were closely related to *Aeromonas* species that have previously been found on *Acartia tonsa* (Tang *et al.* 2009a) and not *Vibrio* spp. that are reported for diverse copepod species (Montanari *et al.* 1999; Tang, Turk and Grossart 2010; Shoemaker and Moisander 2015). However, the single sample from which the *nrfA* PCR amplicon was verified might not be representative for all samples and it can be expected that in a more comprehensive study a larger diversity of *nrfA* associated with copepods in lakes would be revealed.

Oxygen controls on carcass-associated nitrogen cycling

Anaerobic N-cycling associated with the carcasses of *Eudiaptomus* sp. and *M. gigas* was evident even at high ambient O_2 levels, but then the rates were very low compared to the copepod carcasses and algae aggregates investigated in other studies (Glud *et al.* 2015; Klawonn *et al.* 2015; Stief *et al.* 2016; Stief *et al.* 2017). Hypoxic and anoxic incubation conditions stimulated carcass-associated anaerobic N-cycling strongly. Therefore, we assume that the extent of internal O_2 depletion in the studied copepod carcasses was insufficient to allow substantial anaerobic N-cycling at high ambient O_2 levels. This could be due to lack of O_2 diffusion limitation in the relatively small carcasses and/or the low volume-specific O_2 consumption rates during microbial carcass degradation (Schramm *et al.* 1999; Stief and Eller 2006). The internal O_2 levels of the carcasses studied here are not known, but *in situ* O_2 measurements in carcasses of the marine copepod *Calanus finmarchicus* revealed internal anoxia (Glud *et al.* 2015). Even in this relatively large species though, the rates of anaerobic N-cycling (as denitrification) increased strongly with decreasing ambient O_2 level, suggesting a successive expansion of the anoxic center.

The immediate control of anaerobic N-cycling by the ambient O_2 level was observable in carcass incubations during which several anoxic events occurred unintendedly. The carcass-associated microbial communities responded quickly to the onset of anoxic conditions by up-regulating the anaerobic N-cycle pathways DNRA and DNRN, but not denitrification. The latter observation might be due to a low potential for denitrification in the microbial communities colonizing the carcasses, which is consistent with the ~20–400 times lower relative abundance of the *nirS* gene compared to the *nrfA* gene.

Effects of carcass preincubation

Generally, the microbial degradation of zooplankton carcasses is to a large extent driven by bacteria and fungi from the surrounding water that colonize the carcasses within the first day after death (Tang, Hutalle and Grossart 2006; Tang *et al.* 2009b; Bickel and Tang 2010). Thus, much of the bacterial colonization of the copepod carcasses studied here may have occurred during the overnight preincubation. In fact, the carcass-specific bacterial 16S rRNA gene abundance was on average 1.8-fold higher on preincubated than on non-preincubated *M. gigas* carcasses, but statistical significance was narrowly missed ($P = 0.053$). In contrast, the rates of O_2 and NO_3^- consumption, NH_4^+ production, DNRN, and denitrification were all significantly enhanced by the overnight preincubation of *M. gigas* carcasses. An exception to this was the DNRA rate that did not increase during the overnight preincubation, even though the absolute *nrfA* abundance increased on average as much as 4.5-fold ($P = 0.011$). This apparent discrepancy is solved by realizing that DNRA was the only anaerobic N-cycle pathway that showed a high rate also in the non-preincubated *M. gigas* carcasses. Thus, in particular for DNRA, the bacterial populations and suitable microenvironmental conditions were already established on the living copepods.

Microbial community composition

As distinctive microsites in the pelagic zone, copepods and their carcasses host microbial communities that are dissimilar to free-living microbial communities, which was also true for the lake copepods studied here (Tang *et al.* 2009a; Dziallas *et al.* 2013; Bickel, Tang and Grossart 2014; Shoemaker and Moisander 2015; Moisander, Sexton and Daley 2015). The differences in microbial community composition between *Eudiaptomus* sp. and *M. gigas* carcasses were likely explained by those bacterial groups that were already associated with the live copepods, e.g. due to different feeding strategies of the two species (Brandl 2005; Tang *et al.* 2009a). The varying amounts and composition of the food remains in the gut may explain why the same copepod species hosted dissimilar microbial communities (Tang *et al.* 2009a) between different copepod collection days. The overnight preincubation led to a further shift in microbial community composition (and an increase in bacterial abundance; see above), whereas the short-term incubation at different ambient O_2 levels did neither cause shifts in microbial community composition, nor changes in bacterial abundance.

Ecological implications

Microbial carcass degradation and carcass-associated anaerobic N-cycling release DIN into the surrounding water where it can be processed by other microorganisms and thereby influence pelagic N-cycling. For the lake copepods studied here, the main products of carcass-associated anaerobic N-cycling were NH_4^+ and NO_2^-, while N_2 only played a minor role. Additionally, it cannot be ruled out that the carcasses of the lake copepods studied here hosted nitrification activity (i.e. promoting NO_2^- and NO_3^- release into the surrounding water) as shown for the large Arctic marine copepod *Calanus hyperboreus* (Stief *et al.* 2018). Ammonium is released through carcass degradation and carcass-associated DNRA. However, DNRA made up only ~2.5% of the NH_4^+ production by carcass degradation. Under the hypoxic or anoxic conditions in the hypolimnion of lakes, this fraction would increase to ~10%–30%. This raises the question where in a stratified lake the copepod-derived NH_4^+ would make a difference. During periods of stratification, vertical NH_4^+ concentration profiles typically exhibit very low concentrations in the epilimnion and high concentrations in the hypolimnion (Sand-Jensen and Lindegaard 2004; Schubert *et al.* 2006; Hamersley *et al.* 2009). Thus, copepod-derived NH_4^+ is more likely to fuel epilimnetic primary production and nitrification activity (Priddle *et al.* 1997; Lehette *et al.* 2012) than hypolimnetic anammox activity (Schubert *et al.* 2006; Hamersley *et al.* 2009).

Nitrite release through carcass-associated DNRN was of similar quantitative importance and showed the same response to low-oxygen conditions as carcass-associated DNRA. Vertical NO_2^- profiles in lakes rarely exhibit concentrations >0.3 μM throughout the water column (Sand-Jensen and Lindegaard 2004; Schubert *et al.* 2006; Hamersley *et al.* 2009) and thus copepod-derived NO_2^- may relieve NO_2^- limitation of the second step of nitrification in the oxic epilimnion and denitrification and anammox activity in the anoxic hypolimnion of lakes. A rough quantitative estimate on the latter effect can be based

on the copepod abundance in Lake Dagow of 1.8 individuals L^{-1} of which 8% are dead (Bickel, Tang and Grossart 2009), the DNRN rate of *M. gigas* carcasses of 1140 pmol carcass^{-1} h^{-1} measured under anoxic conditions, and the hypolimnetic anammox rates reported for two lakes (i.e. 0.6–21 nM N_2 h^{-1} in a temperate lake (Hamersley *et al.* 2009) and ∼10 nM N_2 h^{-1} in a tropical lake (Schubert *et al.* 2006)). For these two scenarios, copepod-carcass-derived NO_2^- would make up 0.4%–13.9% and 0.8% of the hypolimnetic anammox rate, respectively, which constitutes an indirect contribution to overall fixed-nitrogen loss by sinking copepod carcasses. In an anoxic hypolimnion, denitrification rates can be ∼20 times higher than anammox rates (Wenk *et al.* 2014) and thus the relative copepod contribution to hypolimnetic denitrification would even be lower than to anammox.

Such extrapolations might still overestimate the true copepod contribution to pelagic N-cycling because of the seasonally restricted occurrence of hypolimnetic anoxia and the small volume of the hypolimnion relative to the total lake volume. Additionally, in many lakes, benthic fixed-nitrogen loss is more important than pelagic fixed-nitrogen loss (e.g. Wenk *et al.* 2014) and thus the possible contribution by sinking copepod carcasses to fixed-nitrogen loss is probably small for the overall N-budget of lakes. However, the extrapolation might also underestimate the copepod contribution because much higher relative carcass abundances of up to 40% have been observed in other lakes (Bickel, Tang and Grossart 2009; Elliott and Tang 2009; Tang *et al.* 2014). Finally, also the carcasses of other abundant lake zooplankton, such as cladocerans (Bickel, Tang and Grossart 2009), might contribute to lacustrine fixed-nitrogen loss.

SUPPLEMENTARY DATA

Supplementary data are available at *FEMSEC* online.

ACKNOWLEDGMENTS

We would like to thank Kam W. Tang for fruitful discussions and Anni Glud, Dina Holmgaard Skov, Heidi Grøn Jensen, Lene Dencher, Solvig Pinnow, and Erik Laursen for technical support.

FUNDING

This work was supported by the European Union's Horizon 2020 research and innovation programme (Grant agreement No. 669947; HADES-ERC) and the Danish National Research Council (FNU; 0602-02276B) to RNG and by the German Science Foundation (GR1540/23-1) to HPG.

Conflicts of interest. None declared.

REFERENCES

Avaniss-Aghajani E, Jones K, Chapman D *et al.* A molecular technique for identification of bacteria using small-subunit ribosomal RNA sequences. *BioTechniques* 1994;**17**:144–6.

Bickel SL, Tang KW, Grossart HP. Use of aniline blue to distinguish live and dead crustacean zooplankton composition in freshwaters. *Freshw Biol* 2009;**54**:971–81.

Bickel SL, Tang KW. Microbial decomposition of proteins and lipids in copepod versus rotifer carcasses. *Mar Biol* 2010;**157**:1613–24.

Bickel SL, Tang KW, Grossart HP. Structure and function of zooplankton-associated bacterial communities in a temperate estuary change more with time than with zooplankton species. *Aquat Microb Ecol* 2014;**72**:1–15.

Bonin P. Anaerobic nitrate reduction to ammonium in two strains isolated from coastal marine sediment: a dissimilatory pathway. *FEMS Microbiol Ecol* 1996;**19**:27–38.

Braman RS, Hendrix SA. Nanogram nitrite and nitrate determination in environmental and biological materials by vanadium(III) reduction with chemiluminescence detection. *Anal Chem* 1989;**61**:2715–8.

Brandl Z. Freshwater copepods and rotifers: predators and their prey. *Hydrobiologia* 2005;**546**:475–89.

Cole J. Nitrate reduction to ammonia by enteric bacteria: Redundancy, or a strategy for survival during oxygen starvation? *FEMS Microbiol Letts* 1996;**136**:1–11.

Dalsgaard T, Thamdrup B, Farias L *et al.* Anammox and denitrification in the oxygen minimum zone of the eastern South Pacific. *Limnol Oceanogr* 2012;**57**:1331–46.

Devol AH. Denitrification, anammox, and N_2 production in marine sediments. *Annu Rev Mar Sci* 2015;**7**:403–23.

Dubovskaya OP, Gladyshev MI, Gubanov VG *et al.* Study of non-consumptive mortality of crustacean zooplankton in a Siberian reservoir using staining for live/dead sorting and sediment traps. *Hydrobiologia* 2003;**504**:223–7.

Dziallas C, Grossart HP, Tang KW *et al.* Distinct communities of free-living and copepod-associated microorganisms along a salinity gradient in Godthabsfjord, West Greenland. *Arct Antarct Alp Res* 2013;**45**:471–80.

Elliott DT, Tang KW. Simple staining method for differentiating live and dead marine zooplankton in field samples. *Limnol Oceanogr Methods* 2009;**7**:585–94.

Garcia-Robledo E, Corzo A, Papaspyrou S. A fast and direct spectrophotometric method for the sequential determination of nitrate and nitrite at low concentrations in small volumes. *Mar Chem* 2014;**162**:30–6.

Glud RN, Grossart HP, Larsen M *et al.* Copepod carcasses as microbial hot spots for pelagic denitrification. *Limnol Oceanogr* 2015;**60**:2026–36.

Gorham E, Boyce FM. Influence of lake surface-area and depth upon thermal stratification and the depth of the summer thermocline. *J Great Lakes Res* 1989;**15**:233–45.

Hamersley MR, Woebken D, Boehrer B *et al.* Water column anammox and denitrification in a temperate permanently stratified lake (Lake Rassnitzer, Germany). *Syst Appl Microbiol* 2009;**32**:571–82.

Holmes RM, Aminot A, Kerouel R *et al.* A simple and precise method for measuring ammonium in marine and freshwater ecosystems. *Can J Fish Aquat Sci* 1999;**56**:1801–8.

Kamp A, Stief P, Bristow LA *et al.* Intracellular nitrate of marine diatoms as a driver of anaerobic nitrogen cycling in sinking aggregates. *Front Microbiol* 2016;**7**:Art.1669.

Kirillin G, Grossart HP, Tang KW. Modeling sinking rate of zooplankton carcasses: effects of stratification and mixing. *Limnol Oceanogr* 2012;**57**:881–94.

Klawonn I, Bonaglia S, Brüchert V *et al.* Aerobic and anaerobic nitrogen transformation processes in N_2-fixing cyanobacterial aggregates. *ISME J* 2015;**9**:1456–66.

Kraft B, Tegetmeyer HE, Sharma R *et al.* The environmental controls that govern the end product of bacterial nitrate respiration. *Science* 2014;**345**:676–9.

Lehette P, Tovar-Sanchez A, Duarte CM *et al.* Krill excretion and its effect on primary production. *Mar Ecol Prog Ser* 2012;**459**:29–38.

Liu WT, Marsh TL, Cheng H *et al.* Characterization of microbial diversity by determining terminal restriction fragment length polymorphisms of genes encoding 16S rRNA. *Appl Environ Microbiol* 1997;**63**:4516–22.

Ludwig W, Strunk O, Westram R *et al.* ARB: a software environment for sequence data. *Nucleic Acids Res* 2004;**32**:1363–71.

Lundgaard ASB, Treusch AH, Stief P *et al.* Nitrogen cycling and bacterial community structure of sinking and aging diatom aggregates. *Aquat Microb Ecol* 2017;**79**:85–99.

McIlvin MR, Altabet MA. Chemical conversion of nitrate and nitrite to nitrous oxide for nitrogen and oxygen isotopic analysis in freshwater and seawater. *Anal Chem* 2005;**77**:5589–95.

Moisander PH, Sexton AD, Daley MC. Stable associations masked by temporal variability in the marine copepod microbiome. *PLoS One* 2015;**10**:Art.e0138967.

Montanari MP, Pruzzo C, Pane L *et al.* Vibrios associated with plankton in a coastal zone of the Adriatic Sea (Italy). *FEMS Microbiol Ecol* 1999;**29**:241–7.

Nercessian O, Noyes E, Kalyuzhnaya MG *et al.* Bacterial populations active in metabolism of C-1 compounds in the sediment of Lake Washington, a freshwater lake. *Appl Environ Microbiol* 2005;**71**:6885–99.

Oksanen J, Blanchet FG, Kindt R *et al. Multivariate analysis of ecological communities in R: vegan tutorial.* R package version 1.7. 2013.

Ploug H, Bergkvist J. Oxygen diffusion limitation and ammonium production within sinking diatom aggregates under hypoxic and anoxic conditions. *Mar Chem* 2015;**176**:142–9.

Priddle J, Whitehouse MJ, Atkinson A *et al.* Diurnal changes in near-surface ammonium concentration—interplay between zooplankton and phytoplankton. *J Plankton Res* 1997;**19**:1305–30.

Rusch A, Gaidos E. Nitrogen-cycling bacteria and archaea in the carbonate sediment of a coral reef. *Geobiology* 2013;**11**:472–84.

Sand-Jensen K, Lindegaard C. *Ferskvandsøkologi*. København: Gyldendal, 2004.

Scavotto RE, Dziallas C, Bentzon-Tilia M *et al.* Nitrogen-fixing bacteria associated with copepods in coastal waters of the North Atlantic Ocean. *Environ Microbiol* 2015;**17**:3754–65.

Schramm A, Santegoeds CM, Nielsen HK *et al.* On the occurrence of anoxic microniches, denitrification, and sulfate reduction in aerated activated sludge. *Appl Environ Microbiol* 1999;**65**:4189–96.

Schubert CJ, Durisch-Kaiser E, Wehrli B *et al.* Anaerobic ammonium oxidation in a tropical freshwater system (Lake Tanganyika). *Environ Microbiol* 2006;**8**:1857–63.

Shoemaker KM, Moisander PH. Microbial diversity associated with copepods in the North Atlantic subtropical gyre. *FEMS Microbiol Ecol* 2015;**91**:fiv064

Sorf M, Brandl Z. The rotifer contribution to the diet of *Eudiaptomus gracilis* (G. O. Sars, 1863) (Copepoda, Calanoida). *Crustaceana* 2012;**85**:1421–9.

Stief P, Eller G. The gut microenvironment of sediment-dwelling *Chironomus plumosus* larvae as characterised with O_2, pH, and redox microsensors. *J Comp Physiol B* 2006;**176**:673–83.

Stief P, Behrendt A, Lavik G *et al.* Combined gel probe and isotope labeling technique for measuring dissimilatory nitrate reduction to ammonium in sediments at millimeter-level resolution. *Appl Environ Microbiol* 2010;**76**:6239–47.

Stief P, Kamp A, Thamdrup B *et al.* Anaerobic nitrogen turnover by sinking diatom aggregates at varying ambient oxygen levels. *Front Microbiol* 2016;**7**:Art.98.

Stief P, Lundgaard ASB, Morales-Ramirez A *et al.* Fixed-nitrogen loss associated with sinking zooplankton carcasses in a coastal oxygen minimum zone (Golfo Dulce, Costa Rica). *Front Mar Sci* 2017;**4**:Art.152.

Stief P, Lundgaard ASB, Nielsen TG *et al.* Feeding-related controls on microbial nitrogen cycling associated with the Arctic marine copepod *Calanus hyperboreus*. *Mar Ecol Prog Ser*, 2018, DOI: https://doi.org/10.3354/meps12700.

Tang KW, Hutalle KML, Grossart HP. Microbial abundance, composition, and enzymatic activity during decomposition of copepod carcasses. *Aquat Microb Ecol* 2006;**45**:219–27.

Tang KW, Dziallas C, Hutalle-Schmelzer K *et al.* Effects of food on bacterial community composition associated with the copepod *Acartia tonsa* Dana. *Biol Lett* 2009a;**5**:549–53.

Tang KW, Bickel SL, Dziallas C *et al.* Microbial activities accompanying decomposition of cladoceran and copepod carcasses under different environmental conditions. *Aquat Microb Ecol* 2009b;**57**:89–100.

Tang KW, Turk V, Grossart HP. Linkage between crustacean zooplankton and aquatic bacteria. *Aquat Microb Ecol* 2010;**61**:261–77.

Tang KW, Glud RN, Glud A *et al.* Copepod guts as biogeochemical hotspots in the sea: evidence from microelectrode profiling of *Calanus* spp. *Limnol Oceanogr* 2011;**56**:666–72.

Tang KW, Gladyshev MI, Dubovskaya OP *et al.* Zooplankton carcasses and non-predatory mortality in freshwater and inland sea environments. *J Plankton Res* 2014;**36**:597–612.

Thamdrup B. New pathways and processes in the global nitrogen cycle. *Ann Rev Ecol Evol Syst* 2012;**43**:407–28.

Tian W, Zhang HY, Zhao L *et al.* The relationship between phytoplankton evenness and copepod abundance in Lake Nansihu, China. *Int J Environ Res Public Health* 2016;**13**:1–15, Art.E855

Tiso M, Schechter AN. Nitrate reduction to nitrite, nitric oxide and ammonia by gut bacteria under physiological conditions. *PLoS One* 2015;**10**:Art.e0119712.

Warembourg FR. Nitrogen fixation in soil and plant systems. In: Knowles R, Blackburn TH (eds). *Nitrogen Isotope Techniques*. New York, NY: Academic Press, 1993;157–80.

Welsh A, Chee-Sanford JC, Connor LM *et al.* Refined NrfA phylogeny improves PCR-based *nrfA* gene detection. *Appl Environ Microbiol* 2014;**80**:2110–9.

Wenk CB, Zopfi J, Gardner WS *et al.* Partitioning between benthic and pelagic nitrate reduction in the Lake Lugano south basin. *Limnol Oceanogr* 2014;**59**:1421–33.

Xu Z, Xu YJ. Determination of trophic state changes with diel dissolved oxygen: a case study in a shallow lake. *Wat Environ Res* 2015;**87**:1970–9.

Zehr JP, Mellon MT, Zani S. New nitrogen-fixing microorganisms detected in oligotrophic oceans by amplification of nitrogenase (*nifH*) genes. *Appl Environ Microbiol* 1998;**64**:3444–50.